

Internal Report No. 41  
April, 1983

# Performance and optimization of the Calaid FM system

LIBRARY COPY



NAL

NATIONAL  
ACOUSTIC  
LABORATORIES

COMMONWEALTH  
DEPARTMENT  
OF HEALTH

PLEASE RETURN TO:  
LIBRARY  
NATIONAL ACOUSTIC LABORATORIES  
126 GREVILLE ST  
CHATSWOOD 2067

LIBRARY COPY

NATIONAL ACOUSTIC LABORATORIES  
COMMONWEALTH DEPARTMENT OF HEALTH

NAL INTERNAL REPORT NO. 41

APRIL, 1983

PERFORMANCE AND OPTIMIZATION  
OF THE CALAID F.M. SYSTEM

HARVEY DILLON

(Hearing Aid Research Section)

ACKNOWLEDGEMENT

I would like to thank John Yip for the valuable discussions held during the performance of these measurements and Peter McGilvray for constructing the Kemar voice source.

## CONTENTS

Introduction	1
1. Frequency Response	2
1.1 Methods of measurement	2
1.2 Field surrounding the source	2
1.3 Response with no de-emphasis	4
1.4 Response with single break-point de-emphasis	6
1.5 Effect of noise cancelling microphone on response	8
1.6 Response of hearing aid adaptor	12
1.7 Response of F.M. system and hearing aid	14
1.8 Response with head-worn microphone	17
2. AGC Operation	18
2.1 Compressor input-output function	18
2.2 Analysis of AGC operation	21
2.3 Maximum output level	22
2.4 A.G.C. time constants	26
2.5 Distortion	27
3. VOX Operation	
3.1 Mode of operation of VOX	28
3.2 Measurements of VOX performance	28
3.3 Adjustment of VOX parameters	30
Appendix - Description of the manikin source	35
Bibliography	37

## INTRODUCTION

This report describes measurements performed on "phase II" models of the Cal FM system. Measurements were performed in an acoustically treated audiometric booth using a KEMAR manikin as a sound source, and in an anechoic chamber using a loudspeaker as a source. The KEMAR source was designed to generate a sound field with near and far field directional characteristics similar to those generated by a human speaker. A description is included in Appendix A. This report is divided into sections dealing with the frequency response, AGC operation, and VOX operation of the FM system.

The particular problems of differences in microphone sensitivity, inability to obtain high frequency aided thresholds, and intermittent VOX operation that were mentioned in the report on the field trial of this system, are dealt with in sections 1.8, 2.3, and 3. The measurements described in this report are not intended to provide an exhaustive check on all features of the FM system.

## 1. Frequency Response

### 1.1 Methods of measurement

The CAL FM transmitter incorporates an AGC system. Such systems remove the effect of any frequency dependent networks preceding the AGC monitoring point if sequential test signals, such as swept pure tones, are used. To overcome this, the majority of the testing was performed using broadband input signals, which were then analysed using a Spectral Dynamics SD 360 FFT-based spectrum analyser linked to a HP 85 desk top computer. As KEMAR did not produce a field with a perfectly flat frequency response, a control microphone was employed to measure the field produced as each measurement proceeded. The FFT analyser was used in its transfer function mode, and the displayed results are the ratio of the output of interest to the incident field at the control microphone position. Accuracy of the system was such that the ratio of the outputs of two B & K 4134 microphones located 3 mm apart was within 0.5 dB of a flat response over the range 100 Hz to 10 KHz. When one of the microphones was moved 45 degrees off the source axis (at a distance of 50 mm from the source), the error in the response ratio increased to  $\pm 1.5$  dB over the same frequency range. The control microphone can thus satisfactorily be used at positions up to  $45^\circ$  from the source axis.

### 1.2 Field surrounding the source

The FM transmitter incorporates two microphones, (hereafter called the speech and noise microphones, although of course, both may pick up the same speech or noise signal). Operation of the system is critically dependent on the

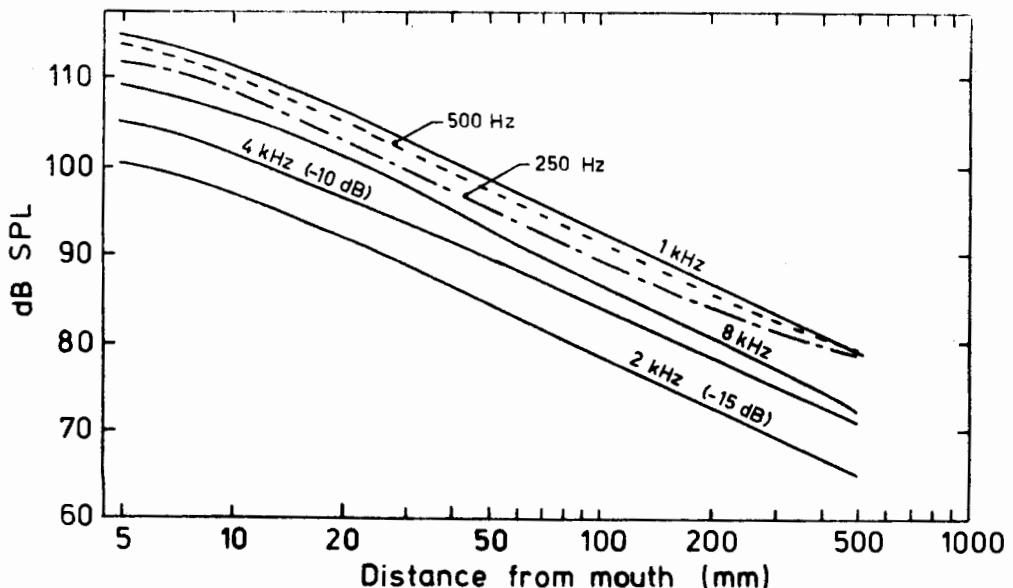


Fig. 1. Field SPL on axis for pure tones of various frequencies.

ratio of the signals at the two microphones. This ratio is determined by the location of the two microphones and the rate of change of field pressure with distance from the mouth. Figure 1 shows the variation of SPL with distance from the mouth. With the possible exception of 8 KHz, an inverse square-law relationship is observed to within  $\pm 1$  dB in the audiometric booth between about 15 mm and 300 mm from the source. As the measuring microphone is moved downwards (on a line between the top of the nose and the sternum on the chest), figure 2

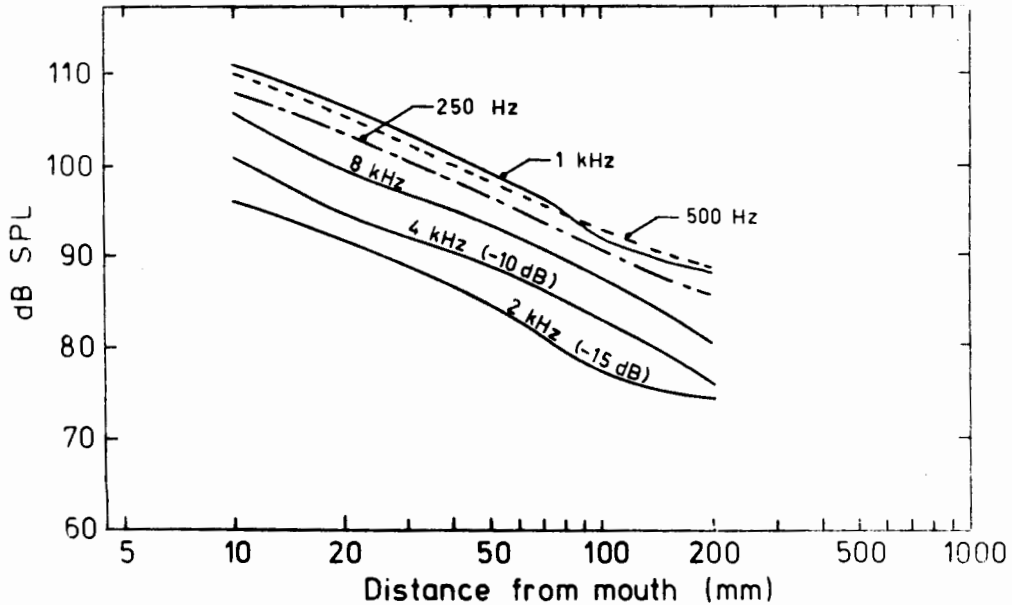


Fig. 2. Field SPL as the measuring microphone moves downward from the mouth.

shows that the inverse square law only applies between approximately 15 and 100 mm, due to reflections off the torso of KEMAR. (If KEMAR is clothed the field conforms somewhat more closely to the inverse square law pattern). Fig. 3 shows the ratio of the field at 15 mm to the field at 100 mm, both on axis. This shows the anomaly of an increased SPL between 6 and 7 kHz in the region surrounding the lips relative to that in the far field. It may be due to a maximum in the imaginary part of the radiation impedance of the tube and lips. The bump appears in all measurements taken with the signal microphone very close to the mouth.

Figure 4 provides us with a check on how well KEMAR simulates the directional characteristics of real people. The solid curve shows the ratio of the SPL at  $45^\circ$  relative to that at  $0^\circ$ , both measured at 100 mm, for KEMAR. The dotted and dashed curves show the corresponding curves for two seated male adults. Some differences are apparent, especially around 800 Hz. These may be caused by reflections from the talker's legs (absent in KEMAR) or some other unknown factors.

Fig. 3. Field SPL 15 mm from the mouth relative to that 100 mm from the mouth.

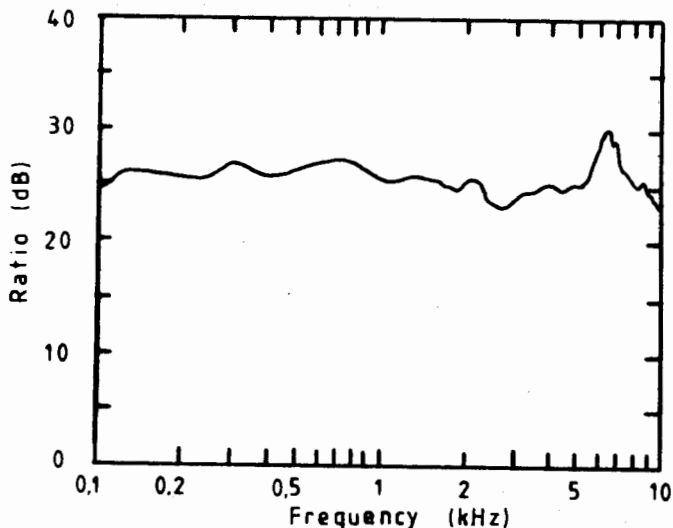
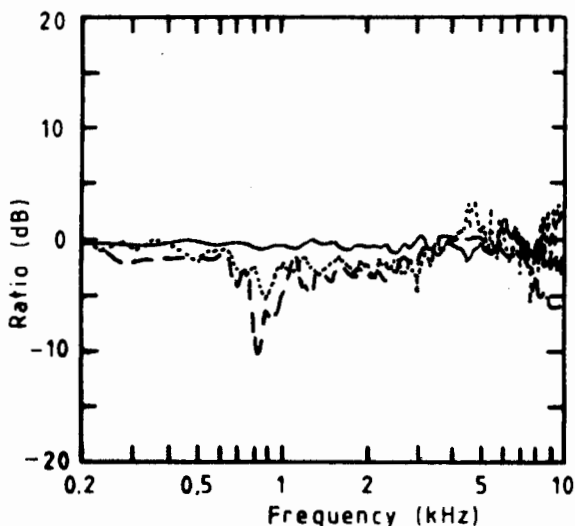


Fig. 4. Field SPL at 45° relative to 0°, both at 100 mm, for KEMAR (solid line) and two male adults.



### 1.3 Response with no de-emphasis

The following measurements, unless otherwise stated, apply to transmitter S/N 200003 operating in the "One Way", "FM", "Channel 3", Power = "H" mode and to receiver S/N 400006 operating in the "FM", "Channel 3", Range = "M" mode. The transmitter and receiver were separated by approximately 1 m and were oriented in the same direction (normally both vertically).

The measurements were initially performed with the transmitter worn around the neck and the boom extended so that the speech microphone was 10 mm directly in front of the lower lip. In this position, the noise microphone is 140 mm from



the mouth. Reference to figures 1 and 2 shows that the noise microphone SPL should be some 22 dB below the speech microphone SPL. Figure 5 shows that the

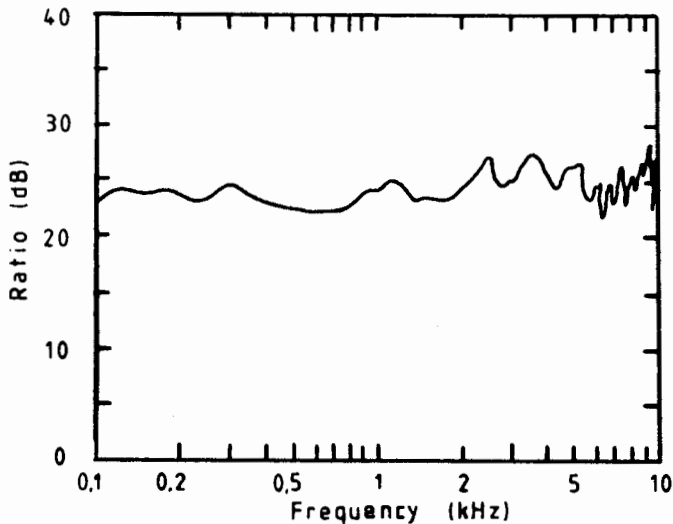


Fig. 5. Field SPL at speech microphone relative to that at noise microphone.

true difference is slightly larger than this and is relatively frequency independent. Such a large difference should ensure that the noise microphone has no effect on the shape of the frequency response. (This is confirmed by the fact that physical attenuation of the noise microphone port has no effect on the measured transmitter-receiver response when worn in this position.)

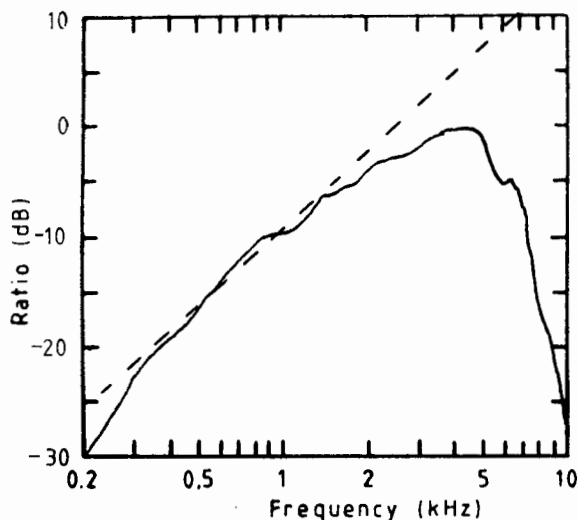


Fig. 6. Response of transmitter and receiver without de-emphasis.

Figure 6 shows the transmitter-receiver response. The response slopes steeply below 500 Hz, then at 6 dB per octave up to 2 kHz, followed by a flat response to 4 kHz, and a steep roll-off above that. Only the behaviour between

500 Hz and 4 kHz is expected from the design specifications of the transmitter. Although it may be thought that the excessively steep low frequency slope is caused by cancellation between the noise and signal paths, this could only occur if the noise path gain exceeds the speech path gain prior to the signal subtractor. This would be contrary to design specification and does not occur because of the agreement between theory and measurements found in section 1.5.

Most of the high frequency roll-off above 4 kHz is accounted for by roll-off in the Knowles BT-1751 microphone used. This could be decreased somewhat by the use of a Knowles EA-1842 microphone, or almost entirely removed by the use of a BT-1753 or BT-1759 (although the latter options would necessitate redesign of the microphone housing block). Use of the Knowles BT-1754 microphone (as fitted to transmitter no.7) is not recommended as the response change at 4.5 kHz is considerably greater than that at 6 kHz and above. The peaked response that would be obtained with the BT-1754 would be harder to flatten with a simple de-emphasis network. Figure 7 shows the boost provided by the BT-1754 and EA-1842 microphones relative to that of the BT-1751.

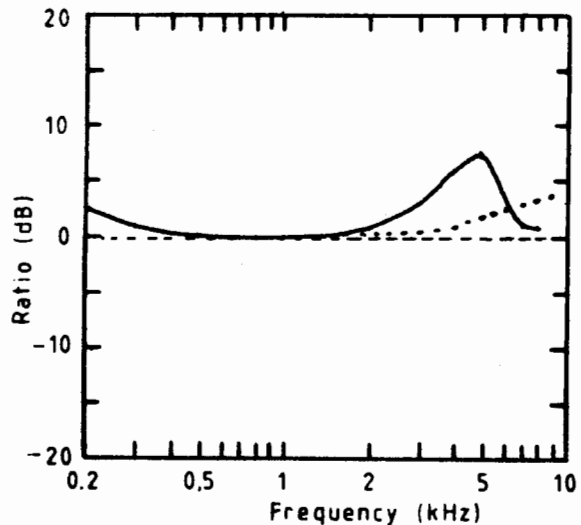


Fig. 7. Response of BT 1754 (solid) and EA 1842 microphone (dotted) relative to that of the BT 1751 microphone.

The transmitter supplied for evaluation contained a foam rubber damper within the boom microphone holder. Figure 8 shows how the presence of this damper affects the response of the system. The decreased sensitivity to high frequencies occurs at and above the microphone resonance.

**RECOMMENDATION:** Foam microphone dampers should not be used. (Note that figures 6 and 8 of this report were obtained with a damper in place).

#### 1.4 Response with single break-point de-emphasis

In order to provide a nominally flat frequency response, the receiver output was connected to a first order low pass filter with a 3 dB break point at 58 Hz. Its transfer function thus slopes down at -6 dB/octave over the entire audio range. The output of the transmitter-receiver-low pass filter combination for

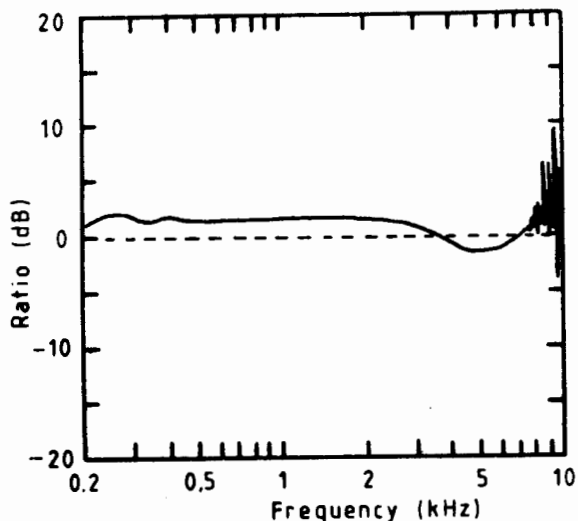


Fig. 8. Effect of foam damper on transmitter response. The raised low and mid frequency response is caused by the modified AGC action.

a range of input levels is shown in figure 9. The input levels range from 40 to 78 dB SPL when measured at 1 m in an anechoic environment, or from 76 to 114 dB SPL at the boom microphone 15 mm in front of the lower lip. Because of the AGC operation, the output remains almost constant over this range of input levels. The frequency response shape deviates from a flat response in just the same way as the previous response deviated from a rising 6 dB/octave response, with the low frequency response 3 dB down at 300 Hz.

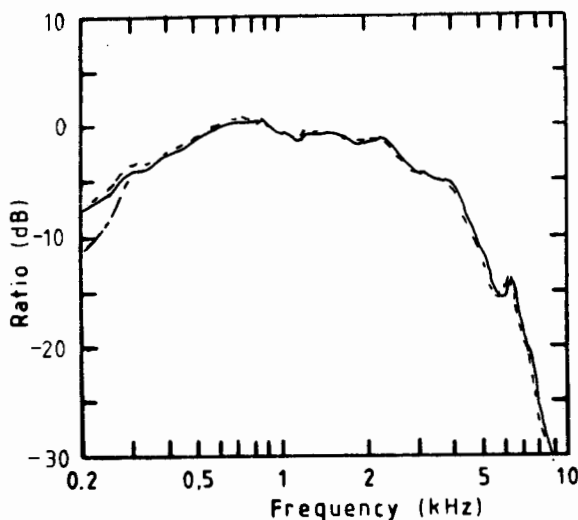


Fig. 9. Response of transmitter, receiver, and single pole de-emphasis network.

For the measurements shown in figure 9, the noise microphone was excluded by

multiple layers of tape. Removal of the tape had less than 1 dB effect on the response, as anticipated from the large difference in signal levels. Measurements were also made with the foam rubber windshield in place. This was found to have no effect on the frequency response.

### 1.5 Effect of noise cancelling microphone on responses

A block diagram of the transmitter audio section which involves the signal and noise transmission paths is shown in figure 10. The speech and noise paths interact in two ways: by subtraction of the noise signal from the speech signal, and by control of the AGC circuit. The latter effect will be considered in more detail in section 2 as it has no effect on the frequency response shape for broad band input signals.

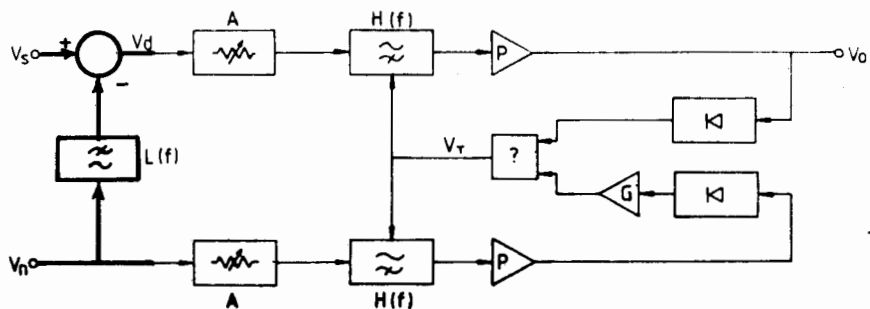
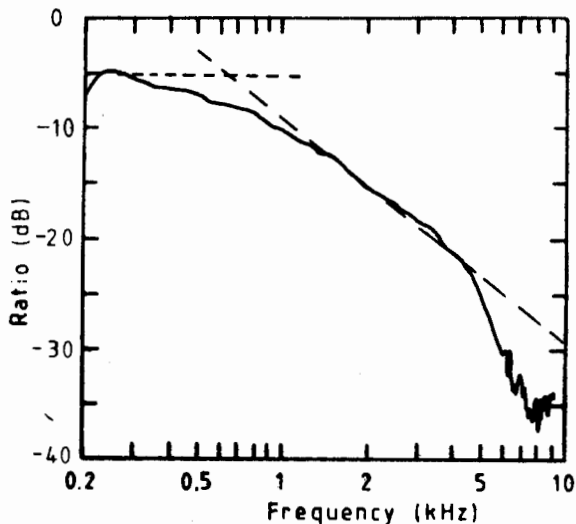


Fig. 10. Block diagram of the input section of the transmitter. Signal subtractor subsection is shown in heavy lines.

A low pass filtered version of the noise is subtracted from the speech signal to give the resulting difference signal,  $V_d$ . Specification for the low pass filter were not available, so the response of the system with the speech microphone blocked was obtained. This is shown in figure 11 and indicates a

Fig. 11. Frequency response of the transmitter and receiver using the noise microphone as input.



break-point at approximately 650 Hz. On a later occasion, the experiment was repeated and the ratio of the noise blocked response to the speech blocked response was obtained. This is shown in figure 12 and indicates a 3 dB

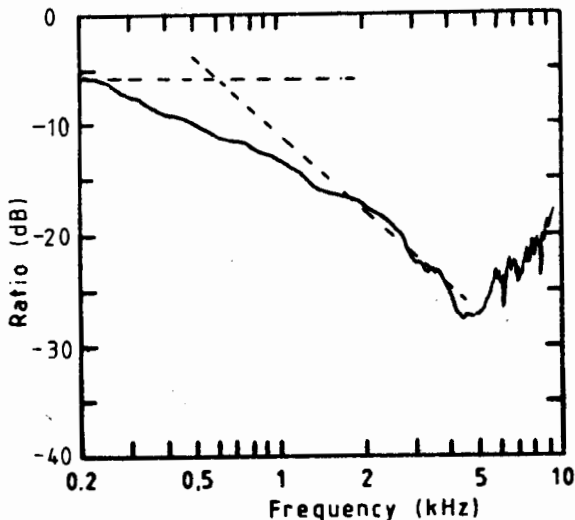


Fig. 12. Ratio of noise path response to signal path response.

breakpoint of around 600 Hz. This figure was adopted for subsequent calculations but has an uncertainty of around  $\pm 30\%$  due to the imprecision with which the asymptotes can be found. (More accurate measurements could be made with electrical signal injection and monitoring of the signal at the output of the subtractor).

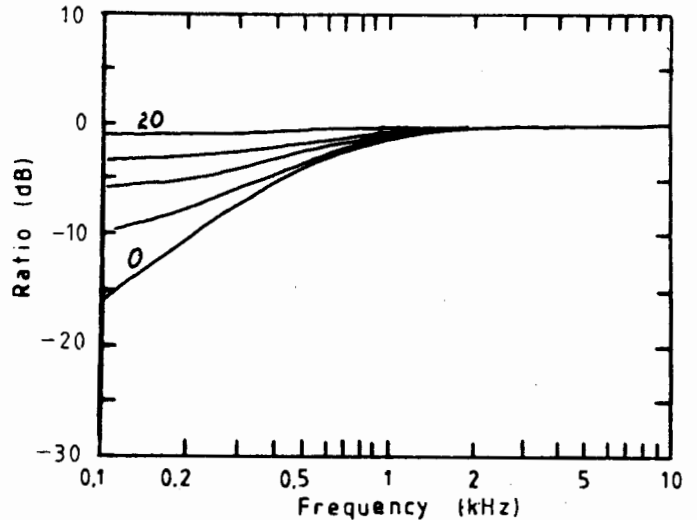
As the "noise microphone" will always pick up some of the acoustic speech signal, it is of interest to find how the subtraction affects the frequency response of the speech path. Firstly, consider the simplified case of the signals at the two microphones being in phase, but with the "speech" signal "b" times larger than the "noise" signal. If the single-pole low pass filter has a break frequency of  $f_0$ , then it is straightforward to show that the ratio,

$$\frac{V_d}{V_s} = \frac{b(1+(f/f_0)^2 - 1 + j(f/f_0))}{b(1+(f/f_0)^2)} \quad \dots 1$$

This is plotted in figure 13 for various differences between the SPL at the speech microphone and the SPL at the noise microphone. The lowest curve shows the suppression that would be expected for a noise signal reaching the transmitter from a far source and travelling in a horizontal plane. The suppression amounts to 15 dB at 100 Hz, and less as frequency increases.

For any other sound source, such as the person wearing or holding the transmitter, a phase difference will exist between the signals reaching the

Fig. 13. Effect of noise cancelling microphone for no acoustic phase shift and speech to noise ratios of 0, 3, 6, 10 and 20 dB.



speech and noise microphones. The phase at the noise microphone relative to the speech microphone is:

$$\theta = -\frac{2\pi f \Delta l}{c}$$

where  $\Delta l$  is the difference in the path lengths from the source to the two microphones and  $c$  the velocity of sound in air. It can then be shown that the effect of the subtractor on the frequency

$$\left| \frac{V_d}{V_s} \right| = \sqrt{1 + \frac{1}{b^2(1+(f/f_0)^2)} - \frac{2 \cos(\theta - \tan^{-1}(f/f_0))}{b\sqrt{1+(f/f_0)^2}}} \quad \dots 2$$

As the inverse square law applies reasonably well over the region likely to be occupied by the two microphones, the ratio  $b$  can be calculated from

$$b = \frac{l_n}{l_s},$$

where  $l_s$  and  $l_n$  are the path lengths from the mouth to the speech and noise microphone respectively. In a typical worn position, these path lengths are 45 and 140 mm. The calculated effect of the subtractor, using these values in equation 2, is shown as the dotted line in figure 14. The firm line shows the measured effect, calculated from the difference between the responses obtained with and without the noise microphone present. The FM system clearly conforms to the expected behaviour. (The slight vertical shift is due to the operation of the AGC system when the noise path is activated.) If the head is then turned by 45°, the path lengths become 100 and 150 mm for speech and noise respectively. The resulting measured and theoretical effects are shown in figure 15. The results in figures 14 and 15 indicate that in these practical worn positions, the only significant deviations in the frequency response occur in the very low frequency region and thus do not represent a significant

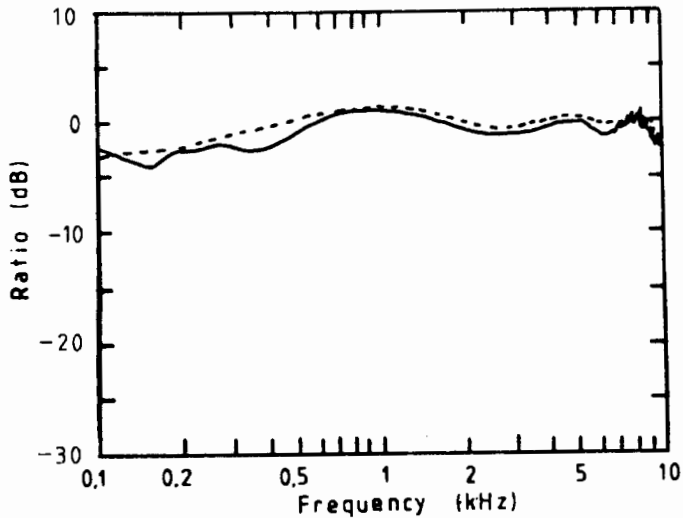


Fig. 14. Measured (solid) and calculated (dotted) effects of the noise-cancelling microphone for speech and noise microphone distances of 45 and 150 mm from the mouth.

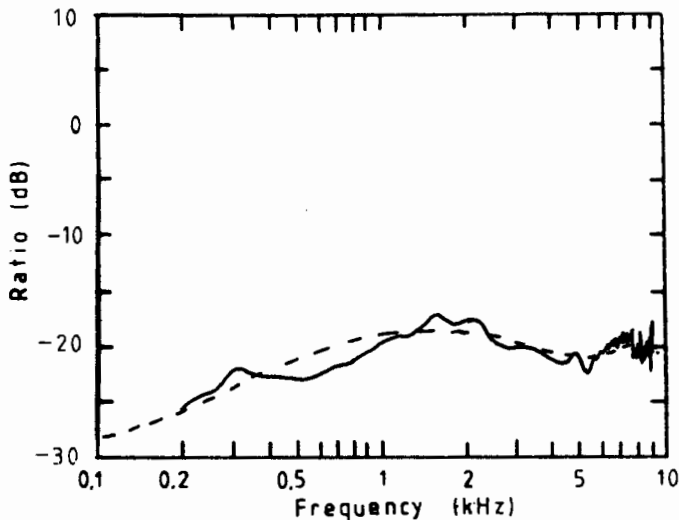


Fig. 15. Same as figure 14 but for speech and noise microphone distances of 100 and 150 mm respectively.

deficiency in the system. Provided the noise microphone is never brought closer to the mouth than the signal microphone, the worst possible situation occurs when the transmitter is held sufficiently far from the mouth that the two signals are approximately equal, and with the path length difference equal to the length of the boom, 150 mm. Figure 16 shows the resulting calculated frequency response. Even in this unlikely situation the notching effect is not huge. At the other extreme, figure 17 shows the small deviations that occur when the speech microphone is located only 25 mm from the mouth.

Fig. 16. Calculated effect of the noise cancelling microphone for equal signals at the two microphones, and a path length difference of 150 mm.

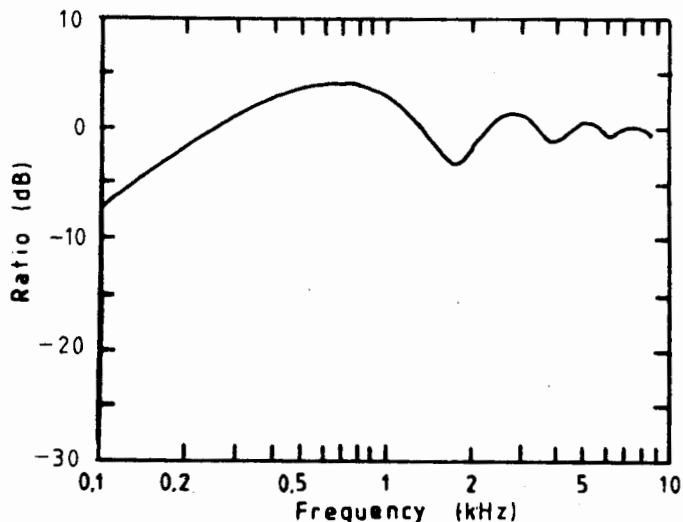
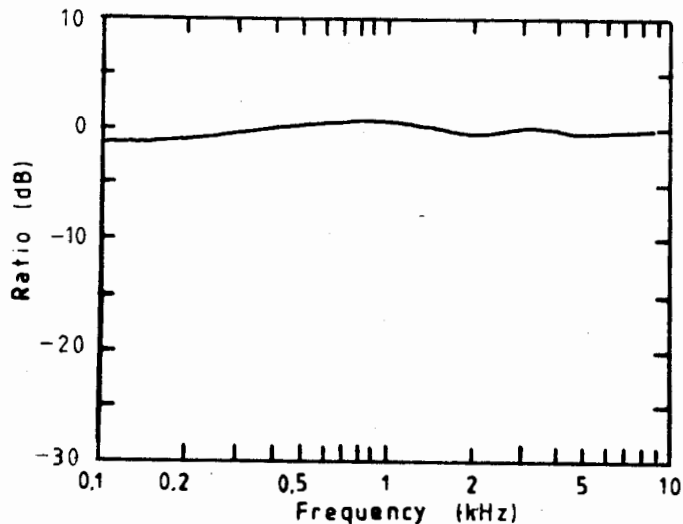


Fig. 17. Calculated effect of the noise cancelling microphone for the speech microphone 25 mm from the lips and the noise microphone 150 mm from the lips.



**RECOMMENDATION:** The notching caused by signal cancellation is not a significant problem, and the cancellation system should be retained because of the low frequency noise suppression it offers. The present low pass filter break point of approximately 600 Hz is well chosen; a lower value would decrease the amount of noise suppression presently provided, while a significantly higher value would cause the frequency response notch effect to increase.

#### 1.6 Response of hearing aid adaptor

It has been proposed that by the use of a special adaptor, the receiver could be coupled to hearing aids not expressly designed to connect to the FM system. The circuit diagram of the adaptor, taken from specification No. FMA-1G, is



shown in figure 18. In order to perform a valid test on the adaptor it must be driven by the correct source impedance and terminated in the correct load impedance. The receiver output impedance was measured and found to vary between  $660\ \Omega$  for an applied signal of 35 mV and  $470\ \Omega$  for an applied signal of 3.5 mV. In the Phonak PPC-2 and PPC-L hearing aids (to which this adaptor is meant to connect), the input impedance is approximately equal to the output impedance of the Knowles EA 1842 microphone and preamplifier. This has a nominal output impedance of  $3.5\ \text{k}\Omega$ . (The measured input impedance of the particular PPC-2 aid used for subsequent testing was found to be  $3.2\ \text{k}\Omega$  and independent of frequency up to at least 4 kHz). Values of  $500\ \Omega$  and  $3.5\ \text{k}\Omega$  were thus adopted for  $R_S$  and  $R_L$  in figure 18.

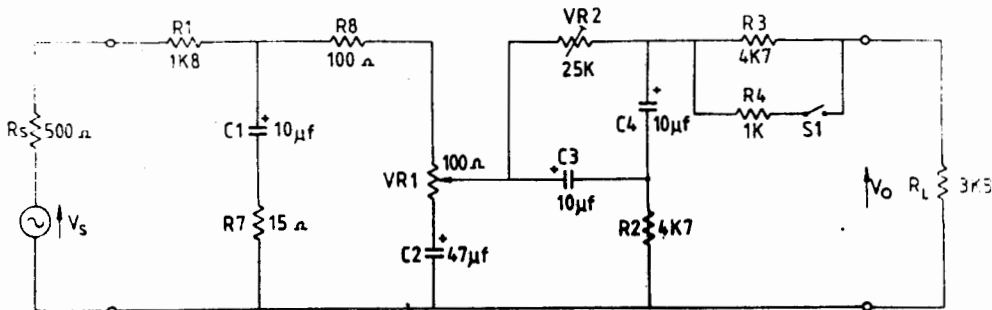


Fig. 18. Circuit diagram of the hearing aid adaptor.

The adaptor fulfils two functions. Firstly, it provides the necessary de-emphasis to restore an overall flat response to the FM system.

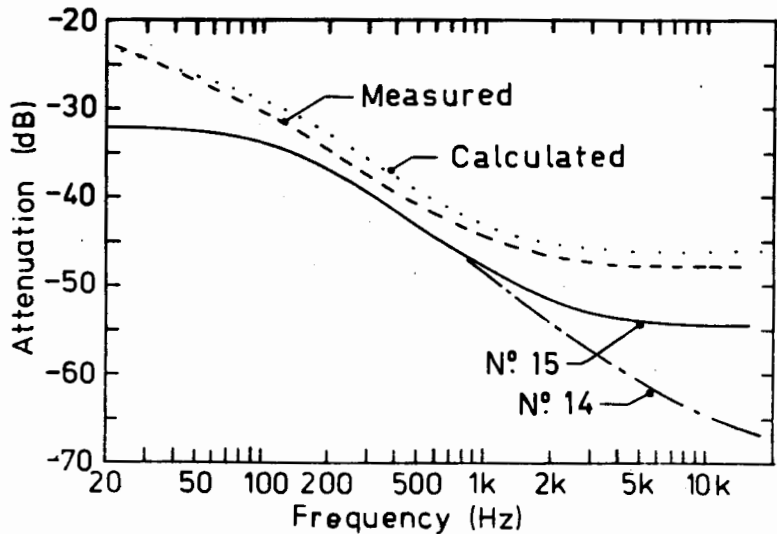
Capacitor  $C_1$  (loaded by  $(R_1 + R_S)/(R_8 + VR_1)$ ) causes the basic roll-off commencing at 80 Hz. The roll-off is terminated at 1100 Hz by  $R_7$ . Capacitor  $C_2$ , in addition to isolating the d.c. component from ground, causes a further roll-off between 1.3 and 70 Hz (which is later modified by the high-pass effect of  $C_3$ ,  $C_4$  and  $VR_2$ ).

The second function of the adaptor is to allow the d.c. level applied by the receiver to the hearing aid microphone to be varied. This has the effect of varying the hearing aid microphone sensitivity. The d.c. level is adjusted by  $VR_2$ . For frequencies above 50 Hz,  $VR_2$  is effectively by-passed by  $C_3$  and  $C_4$  so that it has no effect on the frequency response in the useful hearing aid range.

When switch  $S_1$  is closed, the a.c. signal passed to the hearing aid is increased. Simultaneously, the hearing aid microphone sensitivity is decreased because of the additional d.c. component. The net effect is thus an increase in the ratio of the FM signal to acoustic signal within the hearing aid. The following measurements and calculations were made with  $S_1$  open and  $VR_1$  set to its maximum gain position.

The calculated response of the adaptor is shown as the dashed line in figure 19. The measured response of adaptors number 14 and 15 are also shown.

Fig. 19. Adaptor frequency responses.



A large discrepancy clearly exists between the measured and calculated curves. In the high frequencies, the discrepancy is partly due to the fact that adaptor # 14 has  $R_7 = 0$ , adaptor # 15 has  $R_7 = 10 \Omega$  while the circuit has  $R_7 = 15 \Omega$ . However this should cause the high frequency asymptotic attenuation for adaptor # 15 to be greater than, rather than less than, the calculated value. In order to check the calculations (which were performed with the HP-85 circuit analysis program), the circuit of figure 16 was breadboarded and measured. Its response, shown as the dotted line in figure 19, confirms the theoretical calculations.

Clearly the adaptors, which are similar to those used in the field trial, (with  $R_7 = 0$ ) carried out by Plant and Christen in January 1983, perform differently than ones constructed according to specification No. FM1A-1G. Furthermore the difference involves both the frequency response shape and absolute attenuation of the adaptor. Recommendations about the most appropriate adaptor response will be deferred until section 2.3 of this report.

#### 1.7 Response of F.M. system and hearing aid

The receiver was coupled to a Phonak PPC-2 aid (SN: B2-33882) via the single break point de-emphasis adaptor. To avoid overloading the aid, extra attenuation was added by moving the adaptor break point down to 10 Hz. This brought the signal level at the aid input, for 70 dB SPL white noise into the transmitter, down to 1.06 mV. At the particular mid-volume control setting used (which gave a peak acoustic gain of 47dB), the aid output was then 110 dB SPL which is well within the linear operating region of the aid. The output of the aid alone when set to the "Tone=N, Power=137" switch positions was measured for a 70 dB field level, and then the output of the aid coupled to the FM system (with the noise microphone excluded) was measured. The ratio of these two measurements is shown in figure 20. It can be seen that the FM

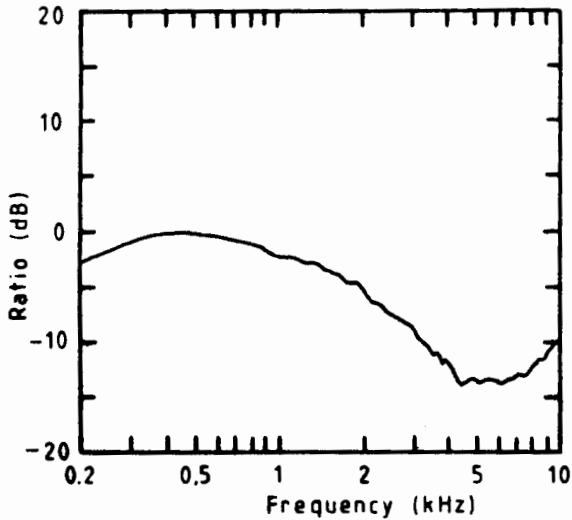


Fig. 20. Effect of the FM system and 6 dB/octave de-emphasis network on the hearing aid response.

system changes the aid's response by rolling off the high frequencies with a break point of approximately 1200 Hz. The 6 dB per octave roll-off ceases at approximately 5 kHz. A small low frequency roll-off also occurs. The origins of this response modification can be seen in figures 21 and 22. Figure 21

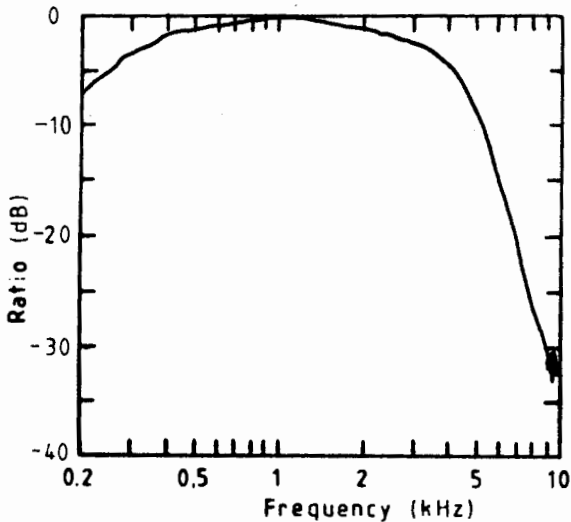


Fig. 21. Response of transmitter, receiver, and 6 dB/octave de-emphasis network.

shows the response of the transmitter, receiver, and single break-point adaptor. Figure 22 shows the ratio of the aid's response when driven electrically to that when driven acoustically (essentially the inverse of the microphone response curve). When these two response shapes are summed the total response modification of figure 20 is obtained.

Fig. 22. Ratio of the PPC-2 aid output for a 1 mV electrical input relative to that for a 70 dB SPL acoustical input.

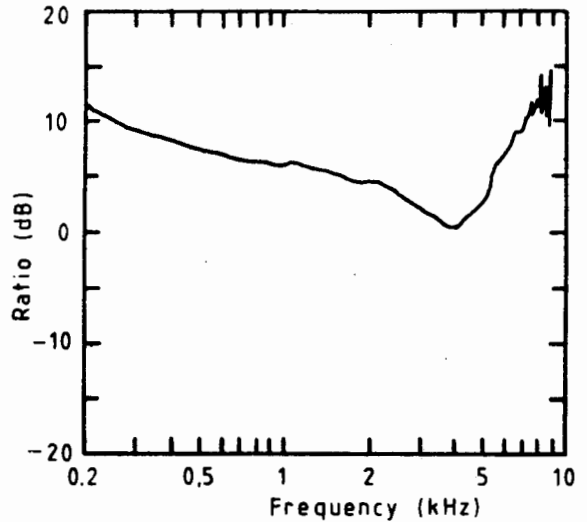
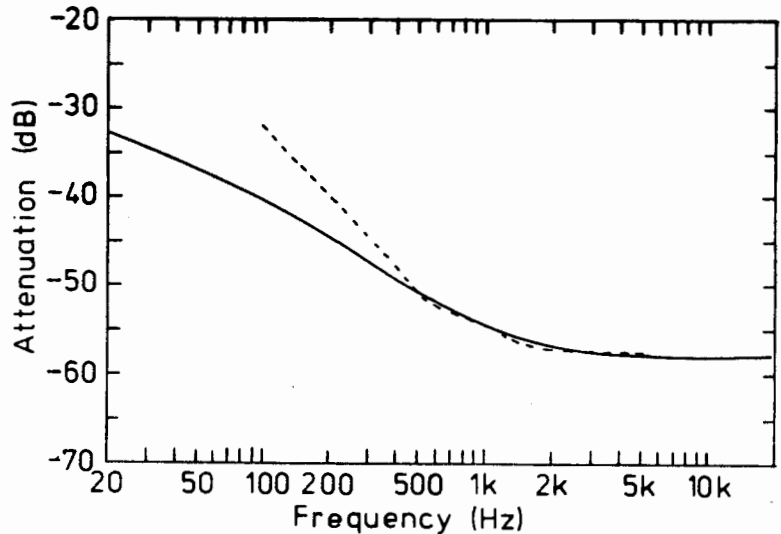


Figure 20 can be used to predict the required adaptor response in order that the aid's response be unchanged by the FM system. This is shown in figure 23, along with the response of the circuit of figure 18. It is evident that

Fig. 23. Adaptor response required to make FM system "transparent" to aid user (dotted). Response of circuit of figure 18 (solid).



in the low frequency region, the desired response would be more closely approximated if the 6 dB/octave slope extended to lower frequencies instead of the more gradual roll-off that is present below 200 Hz.

The system was also measured using adaptor # 15 ( $R_7 = 10\Omega$ ), and the effect on the aid's response is shown in fig 24. For frequencies up to and including 5 kHz, the resulting deviations from a flat response are those which are

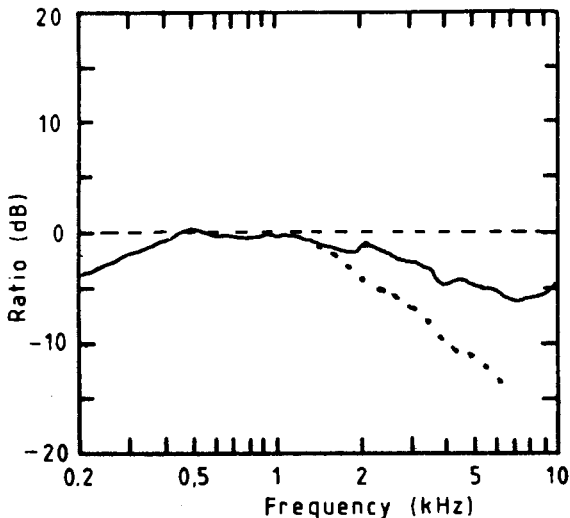


Fig. 24. Effect of the FM system on the hearing aid response when adaptors #14 (dotted) and #15 (solid) are used.

expected based on the differences between the measured response of the adaptor (figure 19) and the desired adaptor response (figure 23). The dotted curve in figure 24 shows the result when adaptor # 14 ( $R_7 = 0$ ) is used. This is nominally the same as the adaptors used in the field trial, and the high-frequency deficiency introduced to the aid by the FM system is then quite marked. Removal of head diffraction causes a further 2dB high frequency loss.

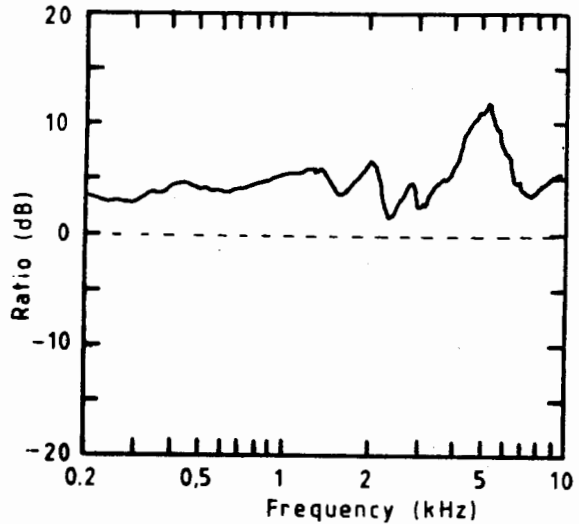
#### 1.8 Response with head-worn microphone

In order to overcome the problem with VOX operation (see section 3), a microphone mounted on a UNISEF headset was used during the field trial in place of the internal boom microphone. The field trial report noted that "the best transmission quality was obtained using the head-worn microphone" and in particular that the high frequency sound /s/ was better perceived using the head-worn microphone.

Consequently, the response of the transmitter and receiver (no adaptor) were measured using both the head-worn microphone and internal boom microphone, and the ratio of the corresponding outputs calculated. The measurements were done with the microphones at both 10 mm and 100 mm from the source, and white noise at both 50 and 100 dB SPL, all with the noise microphone excluded. Figure 25 shows the ratio of the head-worn microphone sensitivity to the boom microphone sensitivity. All responses obtained showed essentially the same shape, although the absolute sensitivity differences were removed by the AGC action at the higher levels tested.

The head-worn microphone is more sensitive than the internal boom microphone at all frequencies, but is especially so around 5 kHz. This is in agreement with the subjective findings. The extra high frequency sensitivity would have partly compensated for the poor high frequency response of the systems used in the field trial (see fig 24).

Fig. 25. Ratio of receiver output using "UNISEF" head-worn microphone to output using internal boom microphone.



## RECOMMENDATION

If it remains necessary to use headworn microphones to ensure reliable VOX operation, some changes will be necessary. Low frequency noise suppression (section 1.5) works most efficiently if the transmission characteristics of the speech and noise paths are well matched, at least below 500 Hz. If different microphone types are used then the auxiliary microphone input circuit should be arranged so that the speech and noise paths have identical low frequency sensitivities, irrespective of whether internal or external speech microphones are used. In addition, the low frequency phase response of the speech and noise microphones needs to be fairly well matched.

## 2 AGC Operation

This section considers the effect that the automatic gain control circuitry in the transmitter has on the output level of the receiver for different signal levels at the speech and noise microphones.

### 2.1 Compressor input-output function

For simplicity, the shape of the input-output function was determined using the speech path only. The noise microphone was excluded and the SPL at the speech microphone varied between 50 and 110 dB. Figure 26 shows the resulting output voltage from the receiver as a function of the input SPL.

The figure shows five curves; one for white noise and one each for pure tones of 200, 500 Hz, 2 kHz, and 5 kHz. For all five curves the output becomes independent of input for high input levels. The system is thus functioning as a limiting type of compressor. As the high pass pre-emphasis occurs prior to the AGC feedback point, the limiting level out of the receiver is approximately independent of frequency. (The slightly lower output level for white

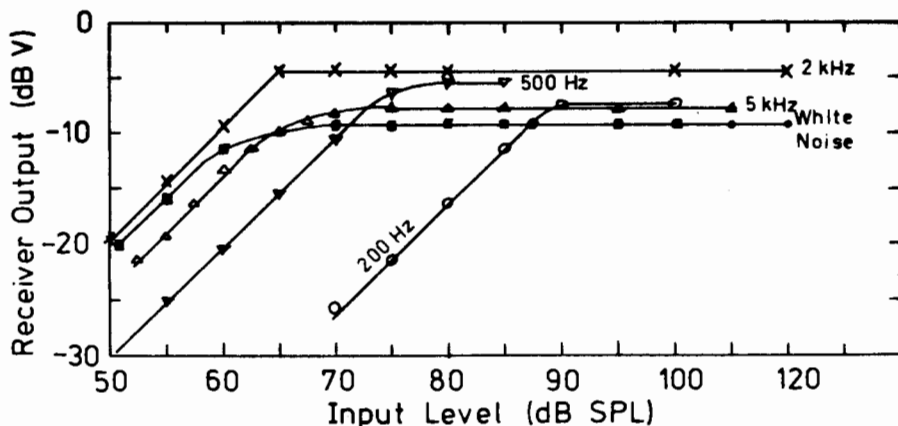


Fig. 26. Input-output curves for pure tones at the indicated frequencies.

noise is partly due to very high frequencies in the white noise which activate the AGC circuit but are then attenuated by later stages of the transmission. It is also caused by the higher peak-to-rms ratio of white noise compared to pure tones). However, the compression threshold referred to the input is strongly dependent on input frequency and should reflect the 2kHz high pass

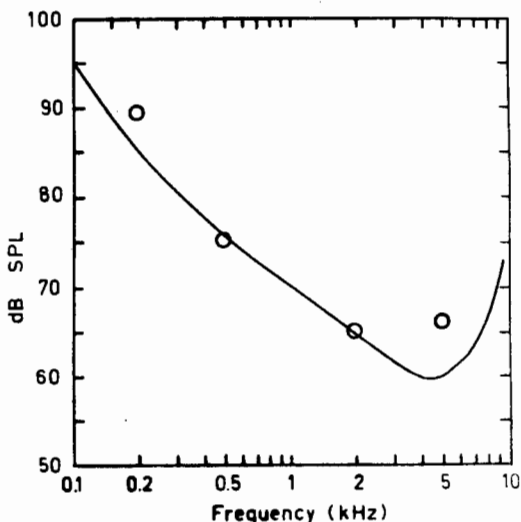


Fig. 27. AGC compression threshold referred to an equivalent input level at the speech microphone.

pre-emphasis characteristic and the microphone sensitivity curve. Figure 27 shows the compression threshold calculated from these two factors (vertical position adjusted arbitrarily), and the measured compression thresholds obtained from figure 26. The two outer frequencies have higher thresholds than expected when compared to the inner frequencies. The discrepancy may

reflect a departure of the microphone sensitivity from its nominal (manufacturer's) characteristic or excessive attenuation at the band edges in the transmitter input circuit.

Figure 29 shows that both the speech and noise paths control the AGC operation. Furthermore, the noise path is given a higher gain than the speech path within the AGC control loop. The purpose of this is to cause a gain reduction whenever the speech and noise signals are equal. It is assumed that under these conditions, the person wearing the transmitter is not speaking. As correct operation of the VOX circuit is critically dependent on the AGC action for different speech microphone signal to noise microphone signal ratios, (SNMR), and as the integrated circuit specifications did not fully detail how the two signals were combined, the AGC action was measured as a function of both signal level and SNMR.

To enable the SNMR to be varied acoustically, the lead to the speech microphone was extended. This enabled the SNMR to be varied over a large range simply by varying the relative distances of the speech and noise microphones from the source. The front of the transmitter case containing the noise microphone was kept at grazing incidence to the incoming wavefront so that diffraction effects around the case were minimised. White noise low pass filtered at 5.5 kHz (to avoid complications caused by the extra 6.5 kHz SPL near the lips) was used as the source signal. Figure 28 shows the receiver output

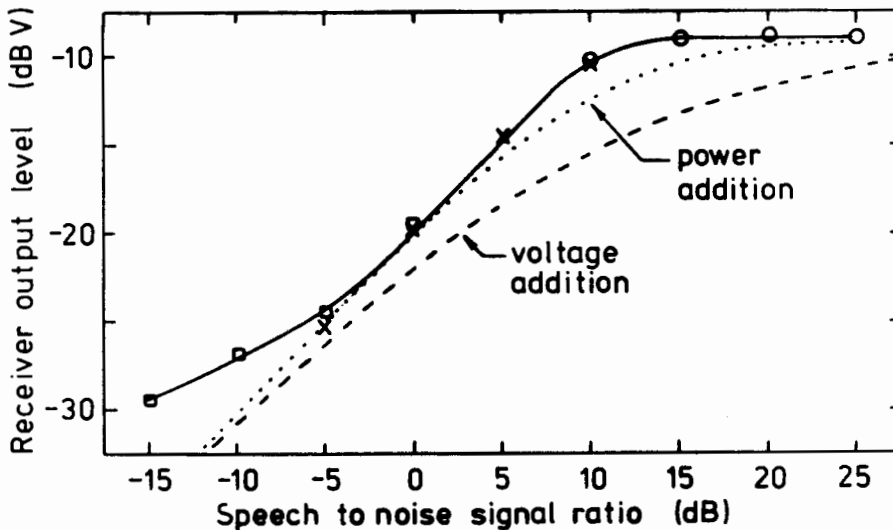


Fig. 28. Receiver output voltage at various speech to noise microphone signal ratios.

(no de-emphasis used) as a function of the ratio of the speech and noise microphone signal levels. The different symbols indicate results obtained at different speech microphone locations. At each of these (20, 100, and 300 mm from the source) the noise microphone was moved to obtain the desired pressure



ratio. For each measurement, the level of the white noise was adjusted so that the circuit was operating in the flat portion of the AGC range, and consequently, the output level was independent of the input level used. The figure indicates that for SNMRs greater than 11 dB, the output level is unaffected by the signal level at the noise microphone, while for SNMRs less than 11 dB, the output level decreases by 1 dB for each 1 dB of decrease in the SNMR. (The deviation from the straight line for very small SNMRs is due to signal originating from the noise microphone entering the speech transmission path via the low-pass filter and signal subtractor and in effect, increasing the SNMR prior to the AGC loop). Furthermore, the changeover between modes is quite sharp. The dashed and dotted curves in figure 28 show, for comparison, the expected behaviour if the rectified speech and noise signals were combined on a power or voltage additive basis respectively. The observed behaviour is much sharper than either of these and corresponds to the circuit choosing as the AGC control voltage the larger out of the signal voltage and 11dB plus the noise voltage. The box labelled "?" in figure 10 can thus be labelled as a "maximum voltage selector", and a value of 3.5 can be assigned to the gain "G".

## 2.2 Analysis of AGC operation

Because of its limiting type compression within the region of operation of AGC, the circuit operates to keep the rectified feed-back voltage  $V_T$  constant, irrespective of the actual SNMR. That is, with reference to figure 29,

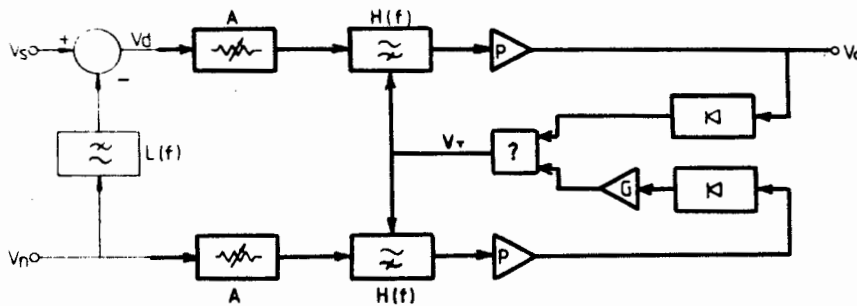


Fig. 29. Block diagram of the transmitter input circuit showing the AGC section in heavy lines.

$$V_T = \text{Max} \left( \left| \frac{V_d}{A} \cdot H(f) P \right|, \left| \frac{V_n}{A} H(f) P G \right| \right) = \text{const} = k \quad \dots 3$$

where A is the attenuation of the voltage controlled attenuators, P & G the gains of the indicated amplifiers, and

$$V_d = V_s - V_n L(f) \quad \dots 4$$

where it is understood that  $V_d$ ,  $V_s$  and  $V_f$  all have frequency dependent spectra. Since A is frequency independent (evidenced by fig. 9) equation 3 can be rearranged to show

$$A = \frac{P \cdot \text{Max} \left( |H(f) V_d|, |H(f) V_n G| \right)}{k} \quad \dots 5$$

The output voltage  $V_O$  can be expressed as

$$V_o = \frac{V_d H(f) P}{A} \quad \dots 6$$

Substitution of equations 4 and 5 into equation 6 gives

$$V_o = \frac{[V_s - V_n \cdot L(f)] H(f)}{\text{Max} (|[V_s - V_n \cdot L(f)] \cdot H(f)|, |GV_n \cdot H(f)|)} \cdot k \quad \dots 7$$

Since  $L(f)$  has a maximum value of 1, and since  $V_n$  is never greater than  $V_s$ , equation 7 can be simplified:

$$V_o(f) = \frac{[V_s - V_n \cdot L(f)] \cdot H(f)}{\text{Max} (|V_s \cdot H(f)|, |GV_n H(f)|)} \cdot k \quad \dots 8$$

From equation 8 we can see that whenever  $V_s \gg V_n$  (speech microphone close to mouth), then  $V_o$  reaches its maximum value  $V_{o\max}$ , where  $|V_{o\max}| = k$ .

When  $V_s$  and  $V_n$  arise from the same source such that  $V_n(f) = V_s(f)/b$ , and when  $V_n \cdot L(f) \ll V_s$  (see section 1.5), then equation 8 can be re-written.

$$V_o = \frac{V_s \cdot H(f) \cdot |V_{o\max}|}{\text{Max} (|V_s|, |V_s \cdot G/b|) \cdot |H(f)|} \quad \dots 9$$

Thus, the gain is reduced by the factor  $G/b$  whenever  $G > b$ . This, of course, is the same result that is displayed graphically in figure 28. Equations 7 to 9 (as appropriate) allow the output expected for any arbitrary combination of speech and noise microphone signals to be calculated. Note that the shape of the frequency response is only affected by the numerator in the equations. Also note that for low signal levels (below the AGC threshold) the denominator takes on a constant value, say  $V_a$ . Equation 8 then becomes

$$V_o = \frac{[V_s - V_n L(f)] \cdot H(f) \cdot |V_{o\max}|}{\text{Max} (|V_s(f)|, |V_n(f)G|, |V_a/H(f)|)} \quad \dots 10$$

Equations 7 and 9 can be similarly modified.

### 2.3 Maximum output level

The report on the field trial indicated that for one subject, aided thresholds could not be obtained above 2 kHz when the FM system was coupled to the aid, even though an aided threshold could be found for the aid alone. One possible reason for this is that the transmitter AGC and the 6 dB/octave deemphasis adaptor combined to limit the input to the aid to a level below that necessary to drive the aid output above the subject's threshold. Figure 30 shows the output of the receiver when the transmitter speech microphone is exposed to a swept pure tone at the indicated levels. The maximum receiver output voltage is approximately independent of frequency; the rounding of the response being imparted by transmitter stages following the AGC monitor point and by the receiver. The maximum voltage out of the adaptor used in the field study can then readily be calculated by subtracting the adaptor attenuation (figure 18) from the receiver output voltage (figure 30). (These results apply for the adaptor switch in the low FM-gain position). Figure 31 shows the results as the solid curve, which indicates that the drive signal to the aid is certainly less for high frequencies than for lows.

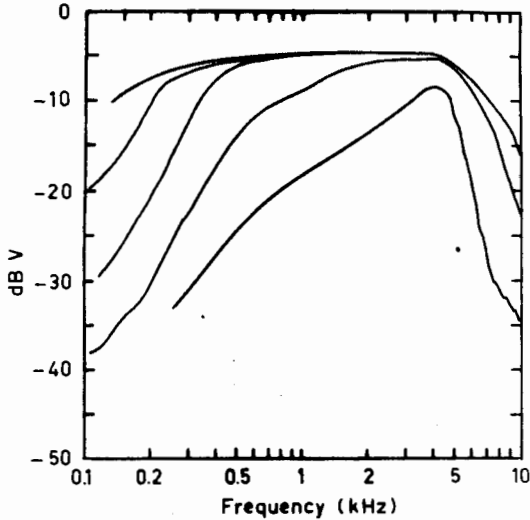


Fig. 30. Receiver output voltage for a swept pure tone input at 60, 70, 80, 90, and 100 dB SPL.

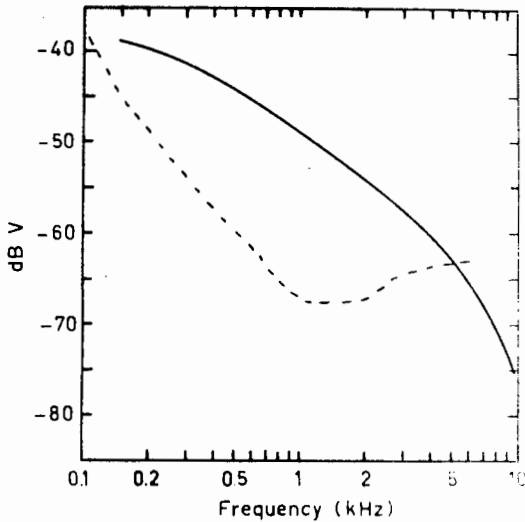
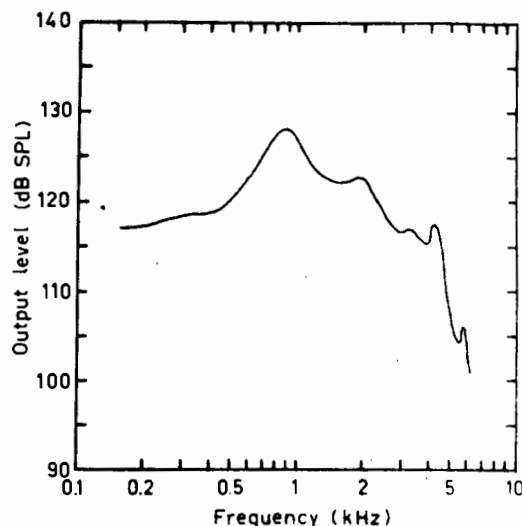


Fig. 31. Maximum level out of the adaptor (solid), and the input level needed to saturate the aid (dotted) for aid settings used in field trial.

However, this curve must be compared with the input needed to just saturate the aid before any valid conclusions can be formed. The dotted curve indicates the required input level for the aid control settings used for the particular subject (MPO=129, Tone=N, V.C.=3.5). Clearly the adaptor output is more than sufficient to saturate the aid for all frequencies below 5 kHz. This was confirmed by comparing the aid output to its OSPL<sub>90</sub> curve for the same control settings. These are shown in figure 32 and are indistinguishable.

Fig. 32. Saturated OSPL<sub>90</sub> curve for the Phonak PPC-2 hearing aid for settings used in field trial.



No explanation is thus offered for why the aided thresholds could be found using the aid alone but not when the FM system was added. The explanation must lie with either an equipment fault not present in the model evaluated or the aid and/or adaptor volume control settings not being set as indicated.

The specific problem mentioned in the field trial report does, however, reflect the more general problem of what the input signal to the aid should be. On the one hand, we do not want the receiver output to be so large that the aid is constantly driven into saturation. On the other hand we do not want the input to be so small that the full output range of the aid cannot be used. Obviously the maximum drive signal at all frequencies can be simultaneously adjusted by use of the adaptor volume control. That is, the solid curve of figure 31 can be shifted vertically downwards. However, its shape cannot readily be changed as it is governed primarily by the de-emphasis characteristic of the adaptor. What shape should the maximum adaptor output curve have? This question is harder to answer. If the purpose of the transmitter AGC were to be activated only for intense acoustic input signals, then the maximum adaptor output curve should parallel the curve showing the minimum input needed to saturate the aid. Unfortunately, this shape is dependent on the tone setting used (eg. fig 33). However in the present FM system, the AGC is activated most of the time and is thus used to keep the aid output at a comfortable level. This implies that all possible input signals should be amplified so that they lie along or close to an equal loudness contour of the impaired hearing aid wearer. The basic rationale of the NAL aid selection procedure is that when the long term average speech spectrum is subdivided into critical bands, all such bands should be amplified to be approximately equally loud. While this is known to break down for severe to profound losses, it does provide a means by which the optimum maximum adaptor output shape can be selected. That is, if the maximum electrical input to the aid provides an input equivalent to the long term speech spectrum when presented acoustically, then any input signal will be amplified to the same loudness level, at least to the degree to which the NAL selection procedure meets its goals.

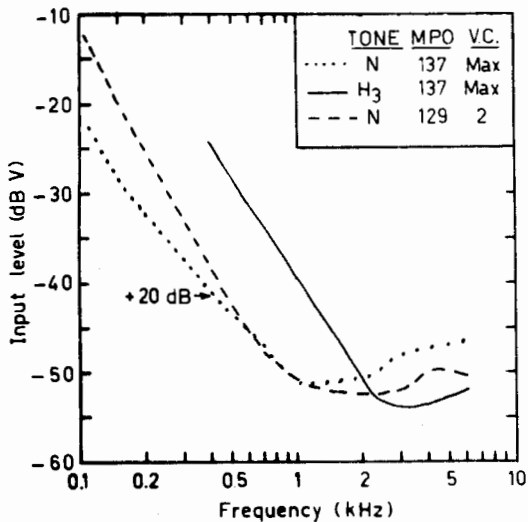


Fig. 33. Electrical input needed to just saturate the aid for several tone, volume, and MPO control settings.

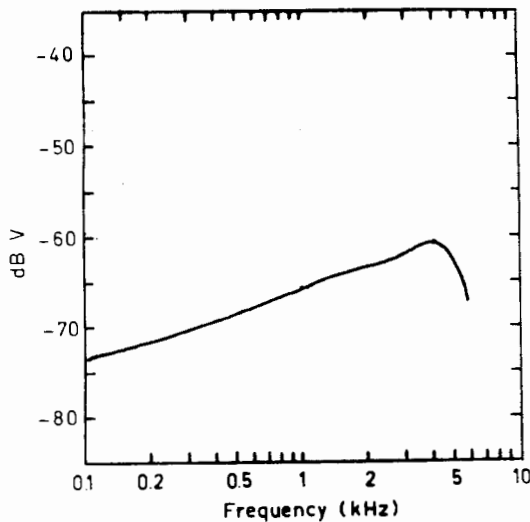
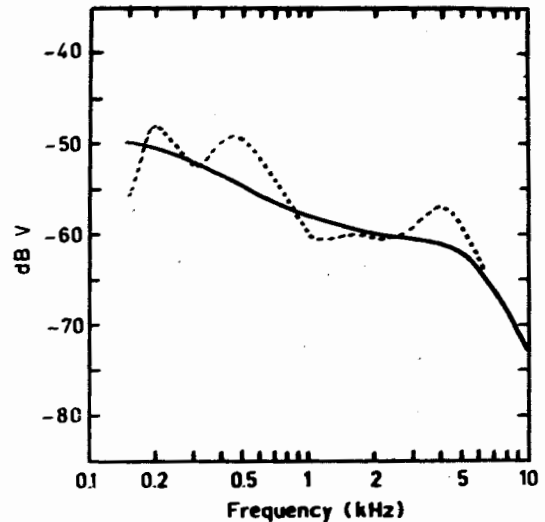


Fig. 34. Electrical input equivalent to an acoustical input of 70 dB SPL.

For the PPC-1 and PPC-2 hearing aids (essentially for the Knowles EA 1842 microphone which they use), the swept pure tone electrical input equivalent to a 70 dB SPL acoustic signal is shown in figure 34. This curve is then used to derive the dotted curve of figure 35 which shows the electrical signal equivalent to an input with the spectrum the same as the long term average speech spectrum (Byrne, 1977). The solid curve shows the maximum input level that would be available using the adaptor of figure 18. The curves are somewhat similar in overall slope and indicate that the existing adaptor specification, as well as providing an approximately flat frequency response

Fig. 35. Electrical input to the aid equivalent to the long term average speech spectrum (dotted) and that provided by the adaptor of figure 18 (solid).



for broad band signals also causes all narrow band signals that exceed the AGC threshold to be amplified to close to an equal loudness contour running through the user's most comfortable listening level. Note that the overall level will be adjusted by the user via the adaptor volume control.

#### RECOMMENDATION:

In section 1.7 it was shown that the FM system would have less effect on the hearing aid's response shape if the adaptor had slightly less attenuation in the low frequencies than that calculated from the circuit of figure 18. The considerations discussed above indicate that the circuit of figure 18 is satisfactory as regards maximum adaptor output level, but figure 35 shows it would be no less satisfactory if the maximum output level at 200 Hz were increased by 3 dB. A slightly better adaptor would thus be one where the 6dB/octave slope extended lower in frequency than it presently does. This is easily accomplished by increasing both R 8 and VR1 in the adaptor to 200 $\Omega$ . In addition, the measurements in this report support the value of 15 $\Omega$  for R7 rather than zero ohms as used in the field trial.

#### 2.4 AGC time constants

The time constants were measured by presenting the speech microphone with a 1 kHz tone that alternated between 80 and 105 dB SPL. The attack and release times (defined as the time taken for the output level to settle within 2 dB of its final level after the input level increases and decreases respectively) were measured on an oscilloscope at 2 ms and 250 ms respectively. The attack time measurement is only accurate to within  $\pm 1$  ms because of distortion in the waveform.

#### RECOMMENDATION:

Based on published data and theoretical considerations (Walker and Dillon,

1982), the release time is somewhat larger than optimum. A release time of 100-150 ms would be preferable. An internal adjustment enables release time to be varied. (Note: 125 ms release time = 184 dB/sec release rate.)

## 2.5 Distortion

As in all systems incorporating pre-and de-emphasis the distortion measured will depend strongly on which type of distortion measure is adopted and where in the system the distortion is measured. In the present system, for example, a swept pure tone input at a level in excess of the AGC threshold will cause the receiver output to remain at approximately 0.5 V over most of the frequency range of interest. Harmonic distortion would then be apparently decreased if the low-pass de-emphasis network was added. The distortion reduction would be illusory, however, since the same network would have the opposite effect of increasing the apparent distortion if intermodulation distortion was measured using high frequency primary tones and low frequency distortion products. In order to avoid this problem, the distortion was measured without the use of the de-emphasis network.

Measurements were made with the use of the NAL 8500 system and the Spectral Dynamics SD360 analyser. The transmitter was placed in one sound attenuating test box, and its speech microphone (on an extended lead) placed in another box. This second box was driven with sound at input levels between 60 and 90 dB SPL, and thus activated only the speech path of the transmitter. The distortion did not change appreciably with input level, indicating that it originates from some point subsequent to the controlled attenuator in the AGC loop. Figure 36 shows the measured second and third harmonic distortion and

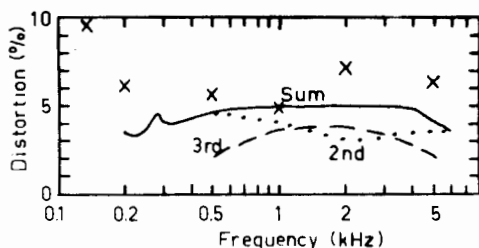


Fig. 36. Second and third harmonic distortion and their power sum, as measured on the NAL 8500 test system. Crosses show sum measurements made on the spectrum analyser.

their sum (on a power basis). Both distortion components are present at comparable levels, with their sum at about 5% over much of the frequency range. Note that the harmonic distortion figures do not decrease sharply in the high frequencies as occurs for measurements on hearing aids. This provides further confirmation that the high frequency response roll-off in the FM system is dominated by the microphone response (which is obviously located prior to the system nonlinearity).

### RECOMMENDATION:

The total harmonic distortion figure of 5% is acceptable but only marginally so. It would be preferable if this figure could be reduced in later versions of the FM systems.

### 3. VOX Operation

The VOX (voice operated switch) portion of the transmitter is designed to sense when the transmitter wearer is talking, and to connect the receiver output to the hearing aid amplifier when this occurs. When the transmitter wearer is not talking, the hearing aid reverts to picking up the acoustic signal at its own microphone. As a result of the field trial and other informal experiments, doubts have been expressed about the efficacy of the VOX feature as it is currently adjusted. In particular, it has been said that the VOX does not appear to switch the transmitter path on unless the speech microphone is held very close to the mouth of the talker. This section describes the mode of operation of the VOX switch, measurements on its performance, and recommendations concerning its improvement if considered necessary.

#### 3.1 Mode of operation of VOX

The VOX sensing mechanism relies heavily on the AGC operation as discussed in section 2.2. Whenever the signal level at the output of the circuit of figure 29 drops below a certain threshold value, the circuit assumes that the talker has ceased. Reference to figures 28 and 26 shows that this occurs whenever the ratio of the signals at the speech and noise microphones (SNMR) drops below a certain value, or when the overall level at the speech microphone drops below the AGC threshold. As section 1.1 showed, the inverse square law (for intensity) applies fairly closely over the region likely to be occupied by the two microphones. Thus, the ratio of the two microphone pressures (and voltages) will be very nearly equal to the ratio of their respective distances from the talker's mouth. Figure 2 shows that, for talker levels above the AGC threshold, correct VOX operation will be assumed provided the speech microphone signal remains 11 dB above the noise microphone signal. This corresponds to a distance ratio of 3.55.

In a typical worn position, the noise microphone is 150 mm from the talker's mouth. Thus, the VOX should switch properly provided the speech microphone is within 42 mm of the mouth. Some additional movement of the speech microphone away from this position should be possible as the VOX will not switch off until the output level has dropped some definite amount below its maximum level.

The next sections consider these points in more detail.

#### 3.2 Measurements of VOX performance

As stated previously, VOX performance is linked with the AGC operation. Since the AGC threshold referred to the input is frequency dependent it was not considered appropriate to use white noise for these measurements. Instead, random noise with a spectrum matched to the long term average speech spectrum for Australian talkers (Byrne, 1977) was used. This was again produced by the KEMAR voice source. Figure 37 shows the input/output curve for the speech spectrum shaped noise with the noise microphone port occluded. The AGC threshold for speech spectrum shaped noise appears to be set at 70 dB SPL. The transmitter was then switched from "FM" to "VOX" and the receiver output observed on a CRO as the input SPL was slowly varied. The VOX threshold, indicated by a change in the d.c. level and the appearance/dis-



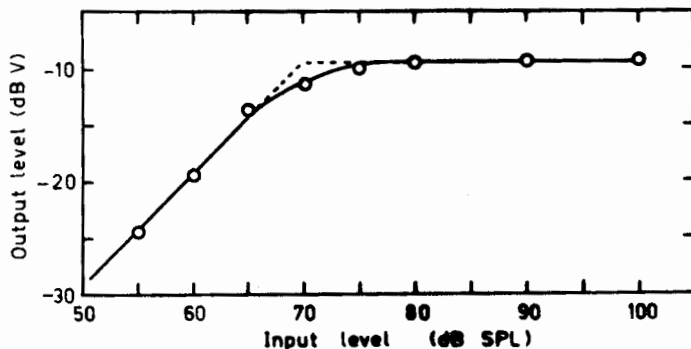


Fig. 37. Input-Output curve using speech spectrum shaped random noise.

appearance of the signal waveform on the CRO, was found to be at 64 dB SPL. Thus, for this particular transmitter, the VOX triggers when the output drops 6 dB below the level set by the AGC loop. Reference to figure 28 shows that, for high input signal levels, this same output decrease also occurs when the speech microphone to noise microphone signal ratio is 5 dB (=11-6). This corresponds to a signal, or distance, ratio of 1.78. Thus, when the noise microphone is 150 mm from the mouth, the VOX should just trigger when the speech microphone is 84 mm from the mouth.

A direct measurement of this critical distance was made by swinging the boom towards the mouth from its folded position. The VOX switched on at a distance of  $75 \pm 5$  mm. The discrepancy between this and the 84 mm calculated above is equivalent to 1 dB of signal level, and is easily accounted for by the accumulated measurement error of figures 28 and 37, and by error in the direct measurement.

We can conclude from these measurements that the VOX is switching in a manner that can be predicted once two basic parameters are known: the critical decrease,  $D$ , in output level (in this case 6 dB), and the gain advantage,  $G$ , that the noise path has over the speech path (in this case 11 dB). Table I summarises the parameters involved in VOX operation.

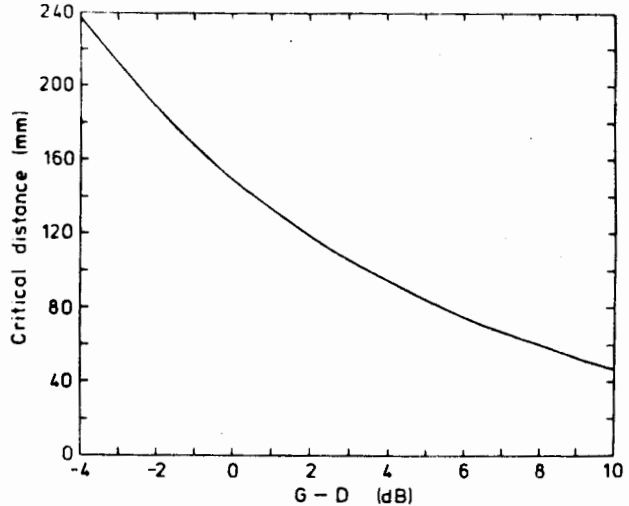
<u>Symbol</u>	<u>Definition</u>
$P_a$	SPL at the noise microphone
$P_s$	SPL at the speech microphone
$P_a$	AGC threshold referred to the SPL of an equivalent speech spectrum shaped signal at the speech microphone.
$G$	Gain advantage (in dB) given to the noise path over the speech path
$D$	Difference (in dB) between the maximum output level and the level at which the VOX circuit just triggers.
$B$	Difference (in dB) between the signal levels at the speech and noise microphones.

TABLE I. Parameters Affecting VOX Performance

### 3.3 Adjustment of VOX parameters.

Based on the previous results it can be seen that there are two obvious ways in which the critical microphone to mouth distance can be increased. These involve an increase in D and/or a decrease in G. The final critical distance depends only on the difference between these quantities, G-D. Figure 38

Fig. 38. The critical distance at which the VOX switches as a function of G-D (see Table I).



shows, for a noise microphone to mouth distance of 150 mm, how the critical speech microphone distance varies as a function of G-D. It is clear that there are no inherent limitations on the critical distance provided the appropriate value of G-D is chosen. Of course, there are other limitations on the range of values that G and D can take, as will be discussed in the following paragraphs. As a design goal, it seems reasonable to ask that the VOX system switch reliably at distances up to 100 mm.

With the speech microphone located just below the lips, and 60 mm from the mouth, a fairly extreme head turn can cause the distance to increase to 125 mm. However, this same head turn increases the mouth to noise microphone distance to 190 mm so that the distance ratio is still equivalent to 100 mm for the speech microphone and 150 mm for the noise microphone.

The effect of varying the different system parameters can best be examined diagrammatically. Figure 39 shows the basic diagram that will be used. It consists of a graph of the sound level (in dB) at the noise microphone versus that at the signal microphone. On the graph is indicated the relative output level of the AGC section of the transmitter. Inspection of equation 10 shows that one of three signals always controls the AGC loop gain: the speech path, the noise path, or the AGC threshold. These correspond to the three regions separated by the heavy lines in figure 39. The lighter lines are contours of constant output level and their variable spacing is meant to indicate that in the two left hand regions (low speech levels), the output level rises with

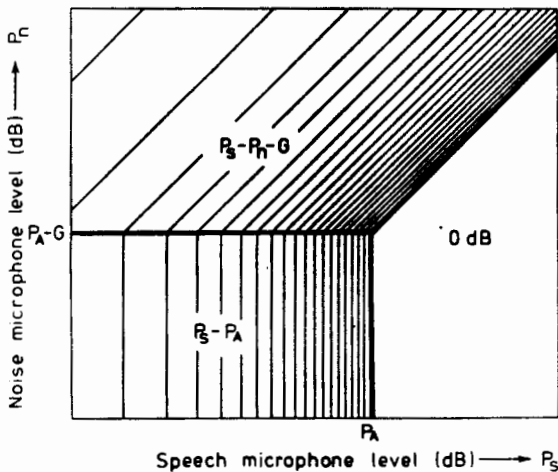


Fig. 39. Output levels for various combinations of input levels at the speech and noise microphones.

input speech level until the right hand region is reached when the maximum output level (of  $-5$  dB V measured at the receiver output) is reached. This is equated to "0 dB" in the figure.

In figure 40, the same graph is drawn but we have now added several new parameters. The dash-dot line through the origin shows the locus of input signals such that the level is equal at the two microphones. Thus, background noise falls somewhere along this line. The dotted line shows the output level necessary to just trigger the VOX. It corresponds to a signal level "D" dB below the maximum output signal. The dashed line at the right shows the locus of input signals originating from the wearer's mouth. Thus, irrespective of the talker level, the speech microphone level is "B" dB above the noise microphone level. The value of B depends only upon the ratio of the two microphone distances from the mouth. To meet our design goal of the VOX triggering at 100 mm speech microphone distance, we require the dashed line to still lie to the right of the dotted curve when  $B = 3.5$  dB. That is, G-D must not exceed 3.5 dB.

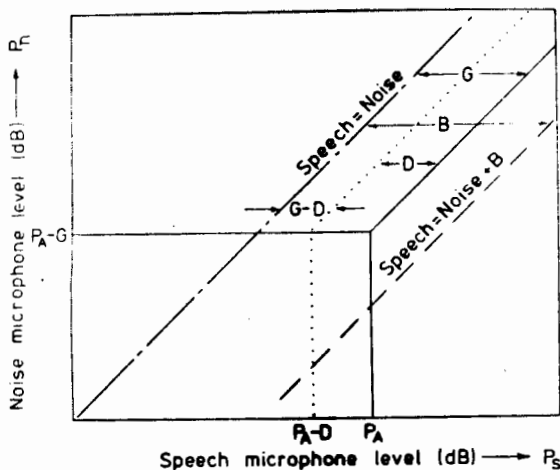


Fig. 40. Similar to figure 39 only showing the relationships, between various parameters defined in the text.

It can be seen from figure 40 that high level background noise results in an output noise level that is only  $G$  dB below the maximum signal level. However, it must be emphasised that this only applies to noise levels in excess of  $P_a - G$ . For lower levels, the signal to noise ratio is equal to  $P_a - P_n$ . We can thus conclude that for good signal to noise ratios at all background noise levels, both  $P_a$  and  $G$  should be as large as possible. The second of these conflicts with making  $G$  smaller to increase the VOX switching distance.

The other change to improve the VOX functioning involves increasing " $D$ ". This moves the dotted curve of figure 40 to the left and so allows  $B$  to be smaller while still keeping the dashed curve to the right of the dotted curve. One obvious limitation to how large  $D$  can be made is that it must always be less than  $G$ . Otherwise  $G - D$  becomes negative and the background noise is sufficient to keep the VOX turned on. To meet this limitation and the design goal of 100 mm microphone distance,  $G - D$  must thus lie between 0 and 3.5 dB. A design figure of 3 dB seems appropriate to allow for production spread as the consequences of a slight reduction in the critical distance are not as great as the consequences of the VOX being permanently turned on by background noise.

However, this has still not answered the question as to what  $G$  and  $D$  individually should be, only what their difference should be. At one extreme, both  $G$  and  $D$  could be made extremely large. The large value of  $G$  ensures that even under high background noise levels, the AGC action does not excessively degrade the perceived signal to noise ratio. The price paid for this is that the VOX will remain switched on over a large range ( $=D$ ) of output levels, and so the hearing aid wearer will hear the talker's voice level fluctuate over that same range as the talker's mouth moves with respect to the speech microphone. While a small fluctuation would not matter, a large fluctuation would move the signal right out of the comfortable listening range for some listeners. At the other extreme, both  $G$  and  $D$  could be made very small. Here the converse applies. The perceived signal to noise ratio for high background levels is deteriorated by AGC action, but the signal level heard by the aid user remains quite constant whenever the VOX is switched on. The lower limit for  $G$  and  $D$  is thus determined by the lower limit for  $G$ , while the upper limit for  $G$  and  $D$  is determined by the upper limit for  $D$ . This is estimated to be about 8 dB but this unfortunately is little better than a guess as no suitable data on this question exists.

One last parameter needs to be considered before these considerations are summarised and conclusions drawn. We have already seen that  $P_a$  should be as high as possible to retain good signal to noise ratios at low background noise levels. The upper limit for  $P_a$  comes from the need for the speech signal to remain above the VOX threshold for the softest speech likely to be encountered (i.e.  $P_s > P_a - D$ ).

This is estimated to be equivalent to a long term rms level of about 75 dB SPL measured 100 mm from the talker's mouth. (This is a fairly conservative estimate given that the average signal level present at an aid wearer's head is usually quoted as about 70 dB SPL).  $P_a$  should thus be set at some value close to but less than 75 dB SPL for speech spectrum shaped noise. The actual choice is somewhat dependent on the value selected for  $D$ .

Table II summarises these considerations. Figure 41 shows the  $P_s$ - $P_n$  plot with the parameters as currently set in the FM aid (in transmitter no. 3, at least). The following can be observed.

- (i)  $P_a$  is far less than the minimum voice level likely to be encountered, resulting in greater signal to noise ratio degradation than necessary.
- (ii) With  $B = 3.5$  dB,  $G = 11$  dB, and  $D = 6$  dB, the dashed curve lies to the left of the dotted curve indicating that the VOX won't trigger at 100 mm speech microphone distance.

<u>Parameter</u>	<u>Lower Limit</u>	<u>Upper Limit</u>
G	Degraded signal to noise ratio for high background noise.	G-D too large; VOX switching distance too small.
D	G-D too large; VOX switching distance too small	Loudness of speech heard by aid wearer fluctuates excessively as the talker moves his head.
G-D	0 so that background noise does not trigger VOX	3.5 dB so that VOX will trigger out to 100 mm microphone distance.
$P_a$	Signal to noise ratio excessively degraded for low level background noise	$P_a$ -D must be less than softest speech sound required to trigger the VOX.

**TABLE II VOX Parameter Constraints**

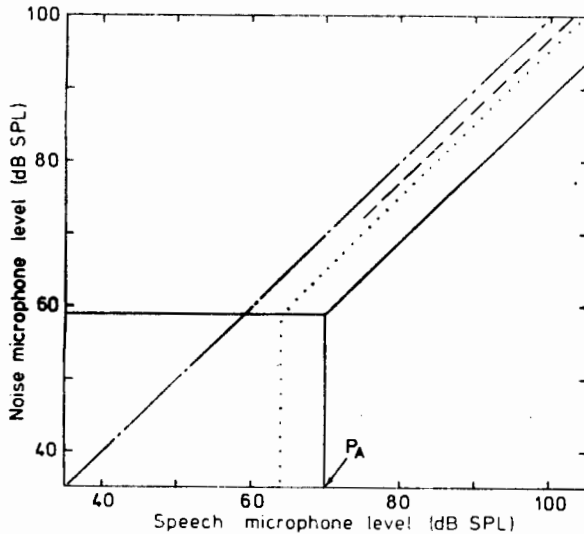


Fig. 41. Relationships between parameters as currently set in the FM aid.

**RECOMMENDATIONS:**

Unfortunately, sufficient basic data do not exist that would enable the optimum parameter values to be specified. We do not know exactly the SPL and spectral shape of the softest sound uttered by a transmitter wearer which is required to trigger the VOX. We also do not know how much fluctuation in output level is tolerable for the aid wearer or what degree of signal to noise ratio degradation is tolerable in the background levels likely to be encountered.

However, based on estimates of these quantities, it is recommended that any subsequent field trials evaluate the following options.

<u>Option</u>	<u>Parameter</u>				
	<u>P<sub>a</sub></u>	<u>G</u>	<u>D</u>	<u>G-D</u>	<u>P<sub>a</sub>-D</u>
1	70	5	2	3	68
2	75	10	7	3	68
3	80	15	12	3	68

These parameter combinations all ensure that all speech spectrum shaped sounds with a level in excess of 63 dB at the speech microphone will just trigger the VOX when the speech microphone is 100 mm from the mouth. Option 1 minimises output level fluctuations, while option 3 minimises SNR degradation. If opportunities do not exist for these options to be field-trialled then the values in option 2 should be adopted. If any of the options lead to the VOX not triggering reliably at distances less than 100 mm, then P<sub>a</sub> will have to be lowered to decrease P<sub>a</sub>-D. If VOX triggering is satisfactory then it is possible that a higher value of P<sub>a</sub> could be tolerated, thus offering a further improvement in signal to noise ratio.

Finally, it is strongly recommended that either G or D be internally adjustable over a small range so that component tolerances can be compensated for, as the value of G-D is quite critical for success of the VOX.

Note: Adjustment of P<sub>a</sub> can also be performed using pure tones. The compression threshold for speech spectrum shaped noise is approximately the same as that for a 1 kHz pure tone.

The acoustic design of the source was based on work performed by Gilman. An unpublished report by Gilman describes a "point source of sound" which is approximated by the use of a copper tube coupled to a horn driver unit. The additional work carried out for those measurements involved the selection of suitable damping material, mounting of the sound source in KEMAR, and design of an electronic response equalizer and overload indicator.

### A.1 Driver and tube

The driver selected was a JBL 2410 mid-range horn driver which was mounted on a bracket inside the torso of KEMAR. Coupled to the driver was a copper tube with an inner diameter of 15 mm. According to papers by Flanagan and Morrow & Brouns cited in the Gilman report (no bibliographic details available) the average mouth opening for a range of phonemes has an area equivalent to a circular piston of diameter 5-13 mm and 17 mm respectively. The tube selected should thus have directional characteristics similar to those of a human voice. The tube, of total length 350 mm, was manufactured with a right angle bend coupler so that the end of the tube could be positioned at KEMAR's mouth. A hole was drilled between KEMAR's lips to accept the tube. The end of the tube was cut in a "V" shape to match the contour of the lips. The frequency response of this system is shown as the upper curve in figure A-1.

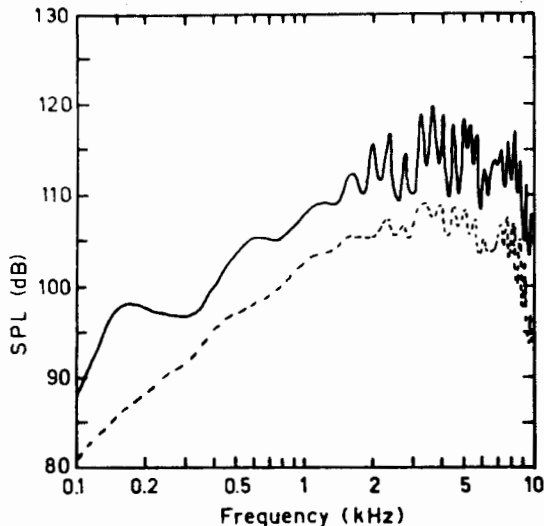


Fig. A1. Output of the KEMAR source before damping (solid) and after damping (dotted) for a 1V input.

### A.2 Damping

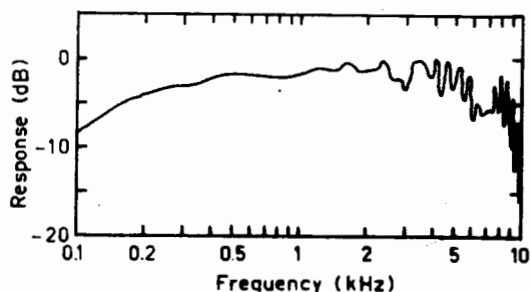
The open end of the tube causes an impedance mismatch which results in the resonant peaks and troughs evident in figure A1. These can be decreased either by terminating the pipe with a resistance equal to the pipe's characteristic impedance, or by internally damping the size of the

resonances. As no suitable terminating resistance was available, the latter option was adopted. The type, amount, and location and density gradient of the damping material were adjusted empirically. Optimum results were obtained with "innerbond wonder-wool" material of dimensions 80 x 25 x 25 mm located in the final 80 mm of the tube. The resulting response, shown as the lower curve in fig A2, was optimum in that the resonance peaks were reduced as much as possible without excessively reducing the output level, especially for the high and low frequencies.

### A.3 Response correction and overload

It is clear that the frequency response of the source is far from flat and requires electronic correction. A reasonably flat response can be achieved by providing a -6 dB/octave boost between 100 Hz and 1.7 kHz. The resulting frequency response is shown in figure A2.

Fig. A2. Response of the KEMAR source with electronic equalization.



The driver unit is rated at 30 W over the range 800 Hz to 15 kHz. This corresponds to a maximum output of 103 dB SPL at 1 m for frequencies above 2 kHz. In addition to the fall-off in level below 2 kHz, the maximum input level must be derated for frequencies below 800 Hz in order to avoid excessive diaphragm displacement. The derating, at 6 dB/octave, should extend down to 100 Hz, where displacement becomes limited by voice coil resistance and mechanical compliance (calculated from impedance measurements at the terminals). A circuit was designed to simulate the necessary derating and a pulse stretcher and overload indicator added. This enables the maximum drive level for complex signals to be readily determined. A complete circuit diagram is shown in figure A-3.

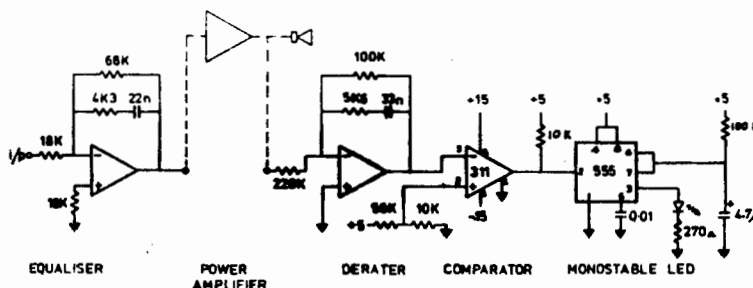


Fig. A3. Circuit diagram of the response equalizer and overload indicator.



### Bibliography

Byrne, D.J. (1977) "The speech spectrum - some aspects of its significance for hearing aid selection and evaluation" Brit. J. Audiol. 11, 40-46.

Plant, G. and Christen, R. (1983) "Field trial of the prototype Calaid FM wireless system 5.1.1983 - 14.1.1983".

Walker, G. and Dillon, H. (1982) "Compression in hearing aids: An analysis, a review and some recommendations" NAL Report No. 90.